



1 **The hydrodynamic and environmental characteristics of tributary bay**  
2 **influenced by backwater jacking and intrusion of main reservoir**

3 Xintong Li<sup>1</sup>, Bing Liu<sup>2</sup>, Yuanming Wang<sup>1</sup>, Yongan Yang<sup>3</sup>, Ruifeng Liang<sup>1\*</sup>, Fangjun  
4 Peng<sup>1</sup>, Shudan Xue<sup>1</sup>, Zaixiang Zhu<sup>1</sup>, Kefeng Li<sup>1</sup>

5 <sup>1</sup> State Key Laboratory of Hydraulics and Mountain River Engineering, Sichuan University, Chengdu 610065, China

6 <sup>2</sup> Emergency Response Centre, Ecology and Environment Bureau of Suining, Suining 629000, China

7 <sup>3</sup> Environmental Monitoring Centre, Ecology and Environment Bureau of Suining, Suining 629000, China

8 **Abstract.** The construction of large reservoirs results in the formation of tributary  
9 bays, and tributary bays are inevitably influenced by the backwater jacking and  
10 intrusion of the main reservoir. The hydrodynamic conditions and the environmental  
11 factors of tributary bays exhibit complex distribution characteristics and  
12 eutrophication occur frequently. Thus, exploring the distribution and evolution of the  
13 hydrodynamic and water environment characteristics of tributary bays in response to  
14 backwater jacking and intrusion is the key to solving eutrophication and other  
15 problems relevant to water environment. In this paper, a typical tributary bay (Tangxi  
16 River) of the Three Gorges Reservoir (TGR) was selected to study the hydrodynamic  
17 and environmental characteristics of the tributary bay influenced by the jacking and  
18 intrusion of the main reservoir. The flow field, water temperature and water quality of  
19 the Tangxi River were simulated using the hydrodynamic and quality model  
20 CE-QUAL-W2, and the eutrophication status of the tributary bay was also evaluated.  
21 The results showed that the main reservoir had different effects on its tributary bay in



22 each month. The tributary bay was mainly affected by backwater jacking of the main  
23 reservoir when the water level dropped and by intrusion of the main reservoir when  
24 the water level rose. An obvious quality concentration boundary existed in the  
25 tributary bay, which was basically consistent with the regional boundary in the flow  
26 field. The flow field and water quality on both sides of the boundary were quite  
27 different. The results of this study can help us figure out how the backwater jacking  
28 and intrusion of the main reservoir influence the hydrodynamic and water  
29 environment characteristics of the tributary bay and provide guidance for water  
30 environment protection in the tributary bays.

31 **Keywords:** tributary bay, main reservoir, backwater jacking, intrusion, hydrodynamic  
32 conditions, environmental factors

### 33 **1 Introduction**

34 The functions of water conservancy and hydropower projects include power  
35 generation, flood control, irrigation and shipping, which play an important role in  
36 human social life (Deng and Bai, 2016; Zhang, 2014; Peng, 2014). In recent years,  
37 with the construction of the Yangtze River Economic Belt and urban agglomeration of  
38 China, a large number of high dams, with heights of over 200 m or even 300 m, have  
39 been planned or completed in the middle and upper reaches of the Yangtze River to  
40 meet the increasing energy demand (Zhou et al., 2013). However, these dams block  
41 the fish migration routes between upstream and downstream regions (Oldani and  
42 Claudio, 2002; Ziv et al., 2012) and change the fish communities (Gao et al., 2010).



43 In the flood season, flood discharge produces water that is supersaturated in dissolved  
44 gas in the downstream river channel (Feng et al., 2014; Lu et al., 2011; Wang et al.,  
45 2011; McGrath, 2006). In the reservoir area, the elevated water level produces a much  
46 slower water velocity, which results in sediment deposition, eutrophication, and  
47 stratification in terms of water temperature and water quality (Zhu, 2017; Wu, 2013;  
48 Zhang et al., 2011).

49 Backwater extends to some tributaries after the construction of dammed-river  
50 reservoirs, which causes the water depth to increase and the water velocity to slow in  
51 these tributaries, thus formed the water areas similar to lakes, and were known as  
52 tributary bay (Yu et al., 2013). Backwater areas represent the connection between  
53 different habitats in the main stream and the tributary and are also an important  
54 location for physical, chemical and biological exchanges between adjacent habitats  
55 (Zhang et al., 2010). After the impoundment of a reservoir, the hydrodynamic  
56 conditions and the environmental factors (water temperature, water quality, etc.) of  
57 the tributaries in the reservoir area are affected by the main stream and exhibit  
58 complex distribution characteristics (Xiong et al., 2013). A tributary bay is always  
59 influenced by backwater jacking and intrusion with the rise of the water level of the  
60 main reservoir because such changes induce changes in the hydrodynamic conditions  
61 in the tributary bay. The velocity of water in the horizontal direction becomes uneven,  
62 and the velocity on the side near the confluence is obviously higher than that on the  
63 other side. The flow field distribution tends to gradually change with increasing



64 distance from the confluence (Yin et al., 2013). The water level of a reservoir changes  
65 constantly to meet multiple requirements, which results in changes in water  
66 temperature and water environment in tributary bays. Existing studies have shown  
67 that water level fluctuation has become a major cause of recent eutrophication and  
68 pollution problems in the TGR, particularly within its tributary backwaters (Holbach  
69 et al., 2015). After the impoundment of reservoirs, eutrophication and  
70 eutrophication-related problems often occur in tributary bays due to changes in  
71 nutrient patterns (Yang et al., 2010; Liu et al., 2012; Ran et al., 2019). Therefore,  
72 exploring the distribution and evolution of the hydrodynamic and water environment  
73 characteristics of tributary bays in response to backwater jacking and intrusion of the  
74 main reservoir is the key to solving eutrophication problems.

75 Many recent studies have paid attention to the deterioration of the water  
76 environment in tributary bays. In response to the operation of cascade reservoirs, a  
77 series of profound geological, morphological, ecological, and biogeochemical  
78 responses will appear in the estuary, delta, and coastal sea of Yangtze River  
79 subaqueous delta (Hu et al., 2009). Some scholars have found that the water quality of  
80 the TGR was relatively stable before and after impoundment but that the water quality  
81 of tributary bays deteriorated, resulting in frequent algal blooms (Liu et al., 2016; Zou  
82 and Zhai, 2016; Cai and Hu, 2006). Changes in the vertical mixing of layers driven by  
83 stratified density currents were the key factor in the formation of algal blooms (Tang  
84 et al., 2016; Zhang et al., 2015). Through isotopic measurements in the Xiangxi River



85 or other tributaries of the TGR, it has been found that the nutrients in tributary bays  
86 did not originate solely in the tributary basins but instead were mainly from the main  
87 stream of the Yangtze River and that the nutrient levels were affected by constantly  
88 changing hydrodynamic conditions across seasons (Holbach et al., 2014; Yang et al,  
89 2018; Zheng et al., 2016). Some scholars found that a rise in the water level may lead  
90 either to a rise in the chlorophyll content or to a decline in the chlorophyll content,  
91 depending on the water cycle mode in the tributary (Ji et al.,2017). The present  
92 studies have paid considerable attention to changes in hydrodynamic characteristics  
93 and the deterioration of the water environment in the tributaries but have not  
94 considered the influence of the main reservoir. There are few systematic studies on the  
95 variation in the hydrodynamic and water environment characteristics of tributary bays  
96 influenced by the backwater jacking and intrusion of the main reservoir. How the  
97 operation of the main reservoir affects the tributary bays, how the hydrodynamic  
98 forces and water environment of the tributary bays respond to the backwater jacking  
99 and intrusion of the main reservoir, what controls the water environment of the  
100 tributary bay? These questions are not yet clear.

101 The Tangxi River, a tributary in the upper reaches of the Yangtze River, was  
102 selected as the focus of this study. The hydrodynamic and water environmental  
103 characteristics of the Tangxi River have inevitably been affected by the backwater  
104 jacking and intrusion of the TGR in recent years. Based on the collection and analysis  
105 of basic data, we simulated the flow field, water temperature, and water quality of the



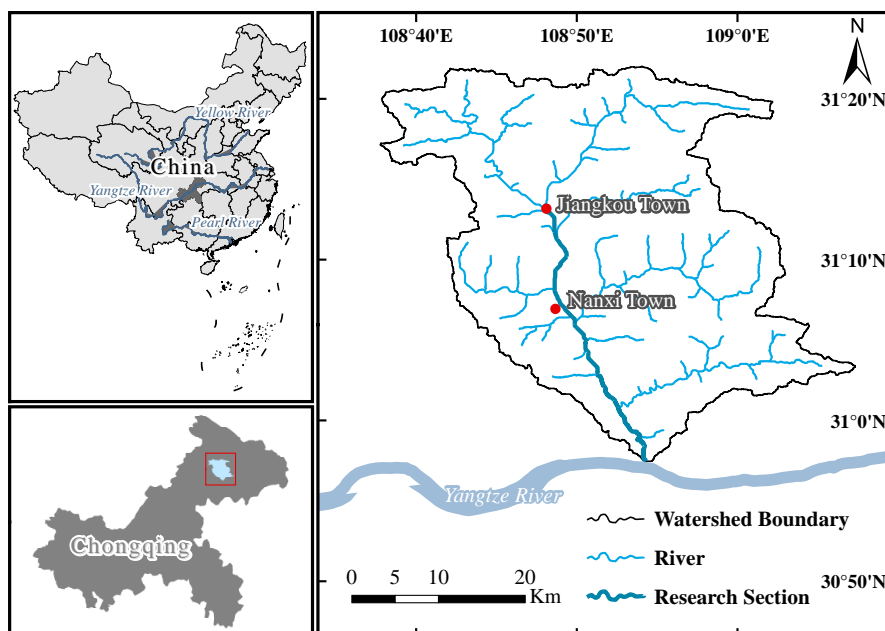
106 Tangxi River using the hydrodynamic and quality model CE-QUAL-W2. Then, we  
107 evaluated the eutrophication status of the tributary bay and systematically identified  
108 the influence of the backwater jacking and intrusion of the main reservoir on the  
109 tributary bay. The results of this study can help us to figure out how the backwater  
110 jacking and intrusion of the main reservoir influenced the hydrodynamic and water  
111 environment characteristics of the tributary bay and provide guidance for water  
112 environment protection in the tributary bays.

## 113 **2 Materials and methods**

### 114 **2.1 Research area**

115 The main stream of the Yangtze River has a total length of approximately 6300 km  
116 and a drainage area of approximately 1.8 million km<sup>2</sup>. The reach between Yichang  
117 City and Hubei Yibin City in Sichuan is considered the upper reaches of the Yangtze  
118 River, which has a length of 1045 km and a natural drop of 220 m. The drainage area  
119 of the upper Yangtze River is 527000 km<sup>2</sup>, and its average annual flow is 14300 m<sup>3</sup>/s  
120 (Fan, 2007).

121 The Tangxi River is a first-order tributary of the upper Yangtze River and has a  
122 total length of 104 km, a drainage area of 1707 km<sup>2</sup> and an average annual flow of  
123 57.2 m<sup>3</sup>/s. After the completion of the TGR, the Tangxi River became a tributary bay  
124 of the TGR. In this paper, the 42.6 km long reach of the Tangxi River affected by the  
125 backwater jacking and intrusion of the TGR was selected as the study area (Fig. 1).



126

127 **Fig. 1.** Research area and hydrologic system of the Tangxi River Basin.

128 **2.2 Numerical simulation of hydrodynamic and environmental factors in the**  
129 **tributary bay**

130 **2.2.1 Mathematical model**

131 The vertical two-dimensional model CE-QUAL-W2 with average width was adopted  
132 for the calculation of the hydrodynamic conditions, water temperature and water  
133 quality in the tributary bay (Thomas and Scott, 2008). This model performs well in  
134 computing the velocity, the intrusion layer at the plunge point, and the travel distance  
135 of the density current (Long et al., 2019), and many scholars have obtained good  
136 results by using this model to simulate the hydrodynamics, water temperature and  
137 water quality of reservoirs and lakes (Debele et al., 2008; Noori, 2015; Long et al.,



138 2018). The model is solved by coupling governing equations, a transport equation and  
139 a surface heat exchange equation.

140 The governing equations of the model are listed as follows.

141 The continuity equation:

$$142 \quad \frac{\partial UB}{\partial x} + \frac{\partial WB}{\partial z} = qB \quad (1)$$

143 The x-momentum equation:

$$144 \quad \frac{\partial UB}{\partial t} + \frac{\partial UUB}{\partial x} + \frac{\partial WUB}{\partial z} = gB \sin \alpha - \frac{B}{\rho} \frac{\partial P}{\partial x} + \frac{1}{\rho} \frac{\partial B\tau_{xx}}{\partial x} + \frac{1}{\rho} \frac{\partial B\tau_{xz}}{\partial z} \quad (2)$$

145 The z-momentum equation:

$$146 \quad \frac{1}{\rho} \frac{\partial P}{\partial z} = g \cos \alpha \quad (3)$$

147 The free water surface equation:

$$148 \quad B_{\eta} \frac{\partial \eta}{\partial t} = \frac{\partial}{\partial x} \int_{\eta}^h UB \, dz - \int_{\eta}^h qB \, dz \quad (4)$$

149 The equation of state:

$$150 \quad \rho = f(T_w, \Phi_{TDS}, \Phi_{ISS}) \quad (5)$$

151 Accurate hydrodynamic calculations require accurate water densities. Water  
152 densities are affected by variations in temperature and the concentration of solids. The  
153 following relationship is used in the model:

$$154 \quad \rho_{T_w} = 999.845259 + 6.793952 \times 10^{-2} T_w - 9.19529 \times 10^{-3} T_w^2 + 1.001685 \times \\ 155 \quad 10^{-4} T_w^3 - 1.120083 \times 10^{-6} T_w^4 + 6.536332 \times 10^{-9} T_w^5 \quad (6)$$

156 where  $x$  and  $z$  represent the horizontal distance and vertical elevation, respectively;  $U$   
157 and  $W$  are the temporal mean velocity components in the horizontal and vertical  
158 directions;  $B$  is the channel width;  $q$  is the discharge;  $t$  denotes the time;  $g$  is the





159 acceleration of gravity;  $\alpha$  is the angle of the riverbed with respect to the  
160 x-direction;  $P$  represents pressure;  $\tau_{xx}$  and  $\tau_{xz}$  are the lateral average shear stress  
161 in the x-direction and z-direction, respectively;  $\rho$  and  $\rho_{T_w}$  represent densities;  $\eta$   
162 and  $h$  are the water surface and water depth, respectively; and  $T_w$  is the water  
163 temperature.

164 The universal transport equation for scalar variables, such as temperature and  
165 chemical oxygen demand (COD), is as follows:

$$166 \quad \frac{\partial B\Phi}{\partial t} + \frac{\partial UB\Phi}{\partial x} + \frac{\partial WB\Phi}{\partial z} - \frac{\partial(BD_x \frac{\partial \Phi}{\partial x})}{\partial x} - \frac{\partial(BD_z \frac{\partial \Phi}{\partial z})}{\partial z} = q_\Phi B + S_\Phi B \quad (7)$$

167 where  $\Phi$  is the laterally averaged constituent concentration;  $D_x$  and  $D_z$  are the  
168 temperature and constituent dispersion coefficient in the horizontal and vertical  
169 directions, respectively;  $q_\Phi$  represents the lateral inflow or outflow mass flow rate of  
170 the constituent per unit volume; and  $S_\Phi$  denotes the laterally averaged source/sink  
171 term.

172 Heat exchange at the water surface includes net solar shortwave radiation, net  
173 longwave radiation, evaporation and conduction. The surface heat exchange is  
174 computed as follows:

$$175 \quad H_n = H_s + H_a + H_e + H_c - (H_{sr} + H_{ar} + H_{br}) \quad (8)$$

176 where  $H_n$  is the net rate of heat exchange across the water surface;  $H_s$  is the  
177 incident shortwave solar radiation;  $H_a$  represents the incident longwave radiation;  
178  $H_{sr}$  and  $H_{ar}$  represent the reflected solar radiation of shortwave and longwave  
179 radiation, respectively;  $H_{br}$  is the back radiation from the water surface;  $H_e$  is the



180 evaporative heat loss; and  $H_c$  represents the heat conduction.

### 181 **2.2.2 Model validation**

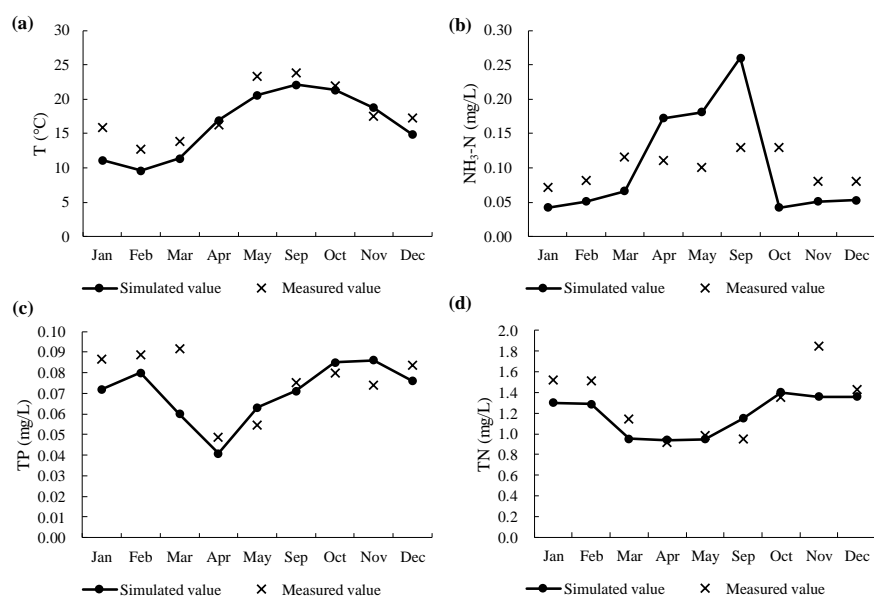
182 The water quality at the Tangxi River Bridge was monitored in 2017, and the data  
183 were used to verify the model. The Tangxi River Bridge is 18 km from the confluence.

184 Due to the low water level of the main reservoir, the backwater did not reach the  
185 Tangxi River Bridge from June to August. Therefore, only the data from January to  
186 May and from September to December were selected to verify the simulated results of  
187 water temperature (T), ammonia nitrogen ( $\text{NH}_3\text{-N}$ ), total phosphorus (TP), and total  
188 nitrogen (TN). COD values were not measured.

189 The results showed that the simulated values of T, TP and TN fit well with the  
190 measured values. The minimum difference in T between the simulated value and the  
191 measured value was 0.6 °C, the maximum difference was 4.7 °C, and the error  
192 percentage between the simulated values and the measured values ranged from 3 -  
193 29%. The minimum difference in TP between the simulated values and the measured  
194 values was 0.004 mg/L, the maximum difference was 0.03 mg/L, and the error  
195 percentage between the simulated and measured values ranged from 5 - 34%. The  
196 minimum and maximum differences in TN between the simulated and measured  
197 values were 0.02 mg/L and 0.26 mg/L, respectively, and the error percentage ranged  
198 from 3 - 38%. For  $\text{NH}_3\text{-N}$ , the differences between the simulated and measured values  
199 were greater than 0.3 mg/L, and the error percentage was greater than 30%. The  
200 degradation process of  $\text{NH}_3\text{-N}$  usually exhibits characteristics and there are many



201 factors affecting the degradation coefficient of  $\text{NH}_3\text{-N}$ , such as the microbial  
202 properties of the water, hydrodynamic conditions, water pollution degree, suspended  
203 solids and pH (Bockelmann et al., 2004; Wang et al., 2016; Pan et al., 2020), which  
204 resulted in a higher simulation error than other values.



205  
206 **Fig. 2.** The comparison between the simulated and measured values at the Tangxi  
207 River Bridge in each month. (a) Comparison of water temperature, (b) comparison of  
208 ammonia nitrogen, (c) comparison of total phosphorus, (d) comparison of total  
209 nitrogen. The points on the graph are simulated values, and the cross marks on the  
210 graph are measured values.

### 211 2.2.3 Boundary conditions

212 The boundary conditions of the calculation included the meteorology, water  
213 temperature of the inflow, discharge flow, water quality and water level of the TGR.



214 The meteorological conditions of the Tangxi River and TGR were based on  
 215 meteorological data from Yunyang County (Table 1), and the pollution loads of point  
 216 and non-point sources were counted and then calculated in this study (Table 2). The  
 217 boundary conditions of flow, water level and water quality are shown in Fig. 3.

218 **Table 1.**

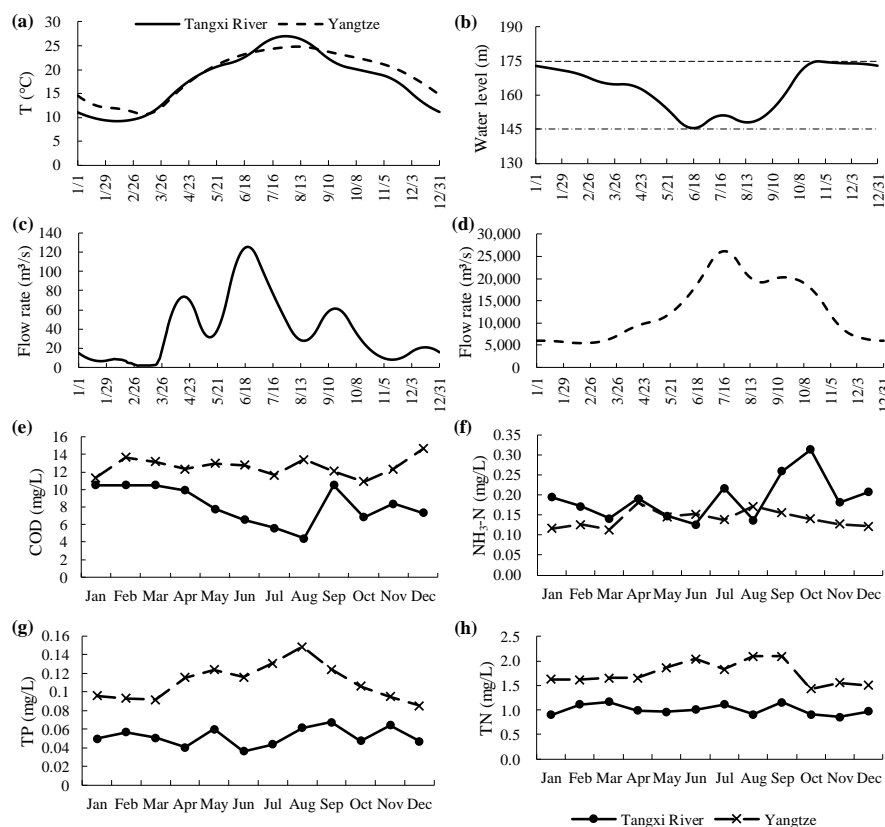
219 Statistical table of meteorological data from the Yunyang meteorological station.

Month	Temperature	Wind speed	Wind direction	Cloudiness	Solar radiation	Relative humidity
	°C	m/s	°	%	W/m <sup>2</sup>	%
1	7.6	0.8	146	81	57.1	78.5
2	9.8	0.9	178	82	74.3	75.8
3	14.3	1.0	165	78	121.2	72.7
4	19.0	1.1	196	75	146.3	74.6
5	22.9	1.1	185	77	149.1	76.9
6	25.8	1.1	198	78	158.7	78.6
7	29.1	1.2	189	68	197.5	72.9
8	29.0	1.2	198	60	203.9	69.4
9	24.7	1.1	216	71	138.3	76.4
10	19.6	0.9	171	78	103.9	81.4
11	14.5	0.8	179	77	73.0	83.0
12	9.1	0.8	172	81	55.5	82.4
Annual	18.8	1.0	183	76	123.2	76.9

220 **Table 2.**

221 Statistics of pollution load in the Tangxi River research area.

Factors	COD (t/a)		NH <sub>3</sub> -N (t/a)		TP (t/a)		TN(t/a)	
	Point	Non-point	Point	Non-point	Point	Non-point	Point	Non-point
Pollution Load	2093.58	1537.35	354.21	154.46	35.08	23.90	2093.58	1537.35



222

223 **Fig. 3.** Simulation boundary conditions. (a) Daily water temperatures of the main  
 224 reservoir and tail of the tributary bay, (b) water level of the main reservoir, (c) daily  
 225 inflow of the tributary bay, (d) daily inflow of the main reservoir, (e) - (h) monthly  
 226 water quality (COD, NH<sub>3</sub>-N, TP and TN) of the main reservoir and tributary bay,  
 227 respectively.

### 228 2.3 Simulation of eutrophication

229 The comprehensive nutrition index (TLI( $\Sigma$ )) method (Carlson, 1977) was used to  
 230 evaluate the nutritional status of the tributary bay. Lakes and reservoirs can be  
 231 classified into different nutritional statuses based on their TLI( $\Sigma$ ) values:



- 232 TLI( $\Sigma$ )<30, oligotrophic  
233  $30 \leq \text{TLI}(\Sigma) \leq 50$ , mesotrophic  
234 TLI( $\Sigma$ )>50, eutrophic  
235  $50 < \text{TLI}(\Sigma) \leq 60$ , slightly eutrophic  
236  $60 < \text{TLI}(\Sigma) \leq 70$ , moderately eutrophic  
237 TLI( $\Sigma$ ) >70, severely eutrophic

238 The formula for calculating the  $TLI(\Sigma)$  is as follows:

$$239 \quad TLI(\Sigma) = \sum_{j=1}^m W_j \cdot TLI(j) \quad (9)$$

240 where  $TLI(\Sigma)$  is the comprehensive nutrition index;  $W_j$  represents the correlation  
241 weight of the nutrition state index of the  $j$ -th parameter; and  $TLI(j)$  denotes the  
242 nutritional status index of the  $j$ -th parameter.

243 Considering chlorophyll-a (chl<sub>a</sub>) as the reference parameter, the normalized  
244 correlation weight formula of the  $j$ -th parameter is as follows:

$$245 \quad W_j = \frac{r_{ij}^2}{\sum_{j=1}^m r_{ij}^2} \quad (10)$$

246 where  $r_{ij}$  is the correlation coefficient between the  $j$ -th parameter and the reference  
247 parameter chl<sub>a</sub> and  $m$  represents the number of evaluation parameters.

248 The correlation coefficients  $r_{ij}$  and  $r_{ij}^2$  between chl<sub>a</sub> and other parameters are  
249 shown in Table 3 (Li and Zhang, 1993).

250

251

252



253 **Table 3**

254 The correlation coefficients  $r_{ij}$  and  $r_{ij}^2$  between chl<sub>a</sub> and other parameters.

Parameter	TP	TN	SD	COD <sub>Mn</sub>
$r_{ij}$	0.84	0.82	-0.83	0.83
$r_{ij}^2$	0.7056	0.6724	0.6889	0.6889

255 The calculation formula of the nutritional status index of each parameter is shown

256 as follows:

257  $TLI(TP) = 10(9.436 + 1.624 \ln TP)$  (11)

258  $TLI(TN) = 10(5.453 + 1.694 \ln TN)$  (12)

259  $TLI(SD) = 10(5.118 + 1.94 \ln SD)$  (13)

260  $TLI(COD_{Mn}) = 10(0.109 + 2.661 \ln COD_{Mn})$  (14)

261 where *TP* is total phosphorus; *TN* represents the total nitrogen; *SD* represents the  
262 Secchi depth, a measure of transparency; and *COD<sub>Mn</sub>* is the chemical oxygen demand.

263 In the parameters above, TP and TN are pivotal. Limitation of one of these, TP or  
264 TN, can limit algae blooms (Bennett et al., 2017; Morgenstern et al., 2015; Lewis et  
265 al., 2011). The nutrient statuses of the surface water in the Tangxi River tributary bay  
266 in different months were evaluated in this study according to the TLI( $\Sigma$ ) method. The  
267 influence of water temperature was also considered during the nutrient status  
268 evaluation.

269

270



271 **3 Results and discussion**

272 **3.1 Hydrological situation**

273 The temporal variations in confluence flow and water level are shown in Fig. 4a.  
274 During July and from August to October, the flow value at the confluence was  
275 negative, which indicated that the tributary bay was mainly affected by backwater  
276 intrusion from the main reservoir. In contrast, the tributary bay was mainly affected  
277 by the backwater jacking of main reservoir in other months (January - June and  
278 November - December). With the water level fluctuation through the whole year, the  
279 backwater intrusion weakened when the water level of the main reservoir dropped,  
280 and when the water level of the main reservoir rose, the backwater intrusion became  
281 obvious.

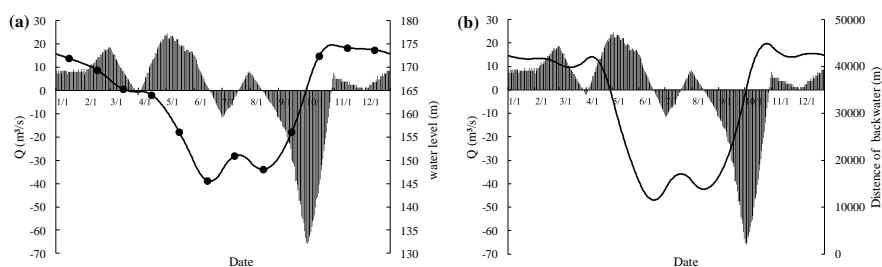
282 The temporal variation in confluence flow and the length of backwater are shown  
283 in Fig. 4b. With the change in the flow at the confluence, the length of backwater also  
284 changed. During January to April and October to December, the water level of the  
285 main reservoir rose to 160 - 175 m, and the backwater reached distances of 39.8 - 42.6  
286 km from the confluence simultaneously. During May to September, the water level of  
287 the main reservoir remained at 145 - 160 m, and the backwater reached distances of  
288 12.6 - 23.8 km from the confluence.

289 The water level and the length of backwater had a negative correlation with the  
290 confluence flow. When the water level dropped, the value of the confluence flow was  
291 positive, and the length of backwater decreased. The tributary bay was mainly





292 affected by the jacking of the main reservoir during this period. Conversely, when the  
293 water level rose, the water flow at the confluence was negative, and the length of the  
294 backwater increased. The tributary bay was mainly affected by backwater intrusion at  
295 this time.



296  
297 **Fig. 4.** The relationships among water level, length of backwater and confluence flow.  
298 (a) Daily variations in confluence flow and water level and (b) daily variations in  
299 confluence flow and length of backwater.

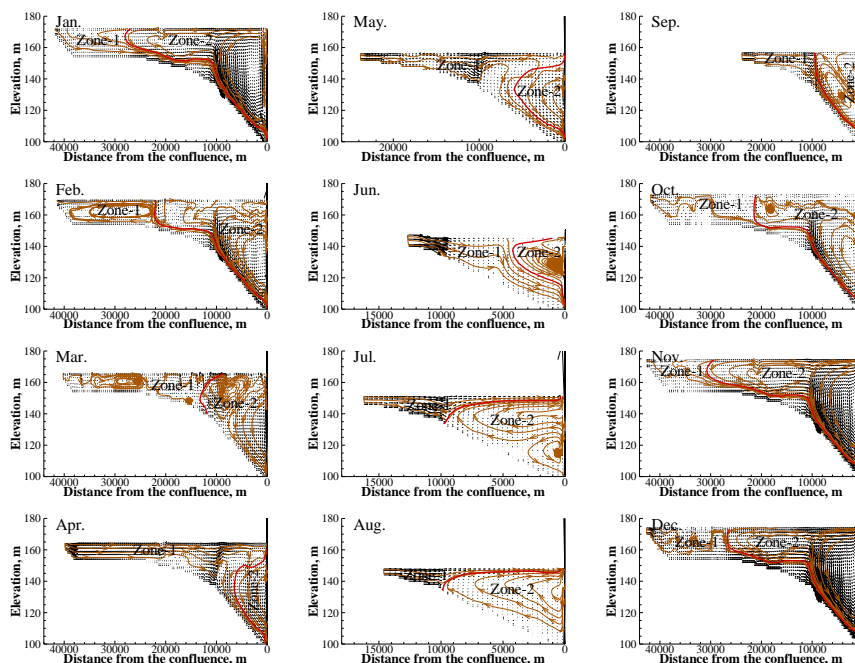
### 300 3.2 Hydrodynamics

301 The distribution of the flow field in each month is shown in Fig. 5. In each month, the  
302 water from the tail flowed along the surface of the tributary bay or sank to the bottom.  
303 The backwater from the main reservoir entered the confluence at different depths  
304 simultaneously, forming one or two flow circulation patterns in the tributary bay.

305 In response to the jacking of the main reservoir in January, the water from the tail  
306 of the tributary bay first flowed along the surface and then sank to the bottom. Under  
307 the influence of geography, the backwater from the main reservoir formed two large  
308 counterclockwise circulations in the tributary bay. The water level gradually  
309 decreased from February to March, and the backwater effect of the main reservoir



310 also gradually weakened. The water from the tail formed one circulation (February) or  
311 two circulations (March) in the tributary bay. From April to June, as the upstream  
312 water of the tributary bay joined the surface layer, the circulation zone disappeared.  
313 The upstream water gradually sank as it neared the confluence, and at the same time,  
314 the backwater from the main reservoir entered the tributary bay in the upper middle  
315 layers and formed a small counterclockwise circulation. From July to August, the  
316 upstream water of the tributary bay directly flowed to the confluence from the surface  
317 layer, and the backwater from the main reservoir entered the tributary bay in the  
318 middle and lower layers, forming one circulation in August and two circulations in  
319 July. In September, the upstream water first flowed through the surface layer and then  
320 sank to the middle of the tributary bay. The backwater from the main reservoir  
321 inclined upward from the lower layer and formed two circulations. The upper  
322 circulation was a smaller clockwise circulation, while the lower circulation was a  
323 larger counterclockwise circulation. The water level increased significantly from  
324 October to December, and the influence of the backwater increased simultaneously.  
325 The upstream water of the tributary bay flowed through the surface layer and then  
326 sank to the bottom.



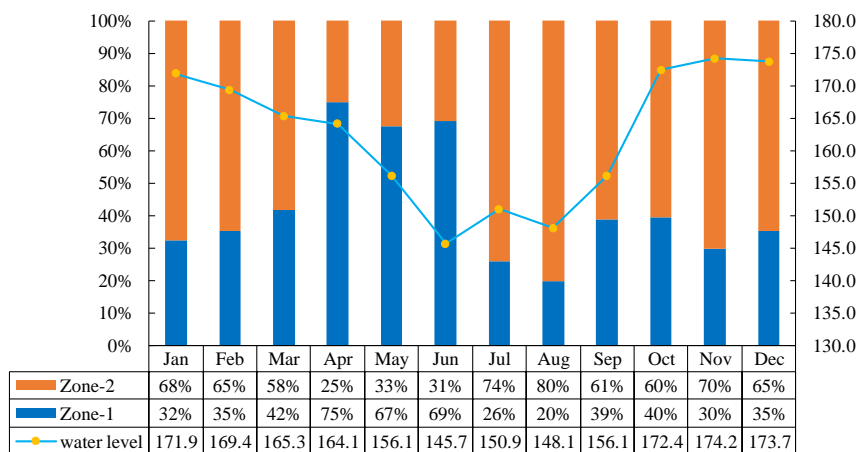
327

328 **Fig. 5.** The distribution of the flow field in each month. The flow field was divided  
329 into two areas (Zone 1 and Zone 2) according to the flow field characteristics. The red  
330 curve in the figure is the boundary between Zone 1 and Zone 2.

331 According to the distribution of the flow field, the tributary bay was divided into  
332 two different areas. Zone 1 represented the area mainly affected by the water from the  
333 tail of the tributary bay, and Zone 2 was the area mainly affected by the backwater  
334 from the main reservoir. Due to the variations in water level and flow value, the  
335 ranges of Zone 1 and Zone 2 differed in each month. The proportions of Zone 1 and  
336 Zone 2 varied with the water level and time (Fig. 6). From January to April, the  
337 backwater reach was from the confluence to Jiangkou Town. With the decrease in the  
338 water levels, the proportion of Zone 1 increased, while the proportion of Zone 2



339 decreased. From May to September, the length of backwater decreased, and it only  
 340 reached Nanxi Town. With the fluctuation in the water level in these months, the trend  
 341 of the proportions of Zone 1 and Zone 2 became irregular. From October to November,  
 342 with the rise in the water level, the proportion of Zone 1 decreased, while the  
 343 proportion of Zone 2 increased. The opposite results were obtained from November to  
 344 December when the water level gradually decreased. From October to December, the  
 345 backwater again reached Jiangkou Town. These results suggested that the backwater  
 346 had a greater impact on the tributary bay when the main reservoir was at a high water  
 347 level and had a smaller impact when the main reservoir was at a low water level.



348

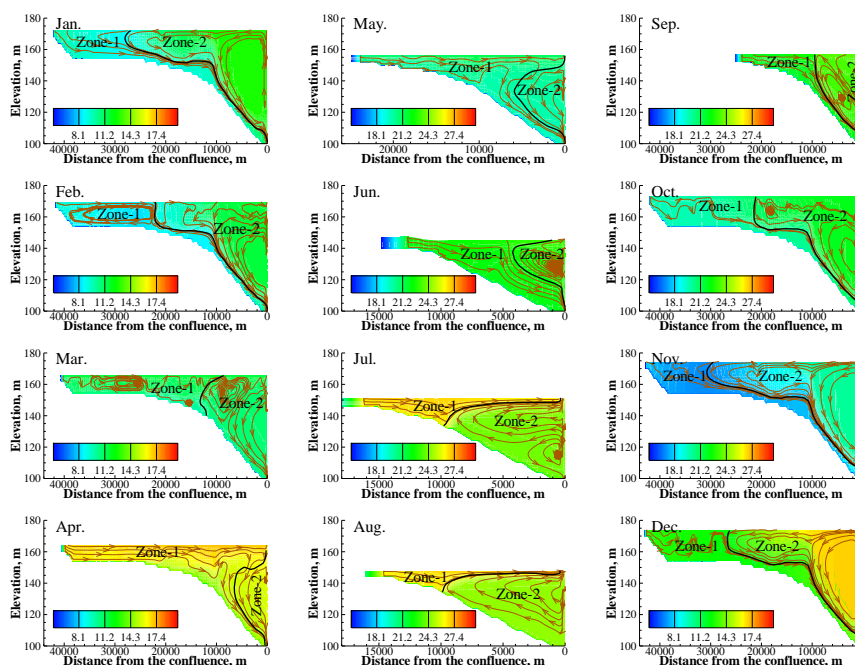
349 **Fig. 6.** The proportions of Zone 1 and Zone 2 and the variation in water level. The  
 350 orange bar represents Zone 2, and the blue bar represents Zone 1. The blue dashed  
 351 line represents the variation in water level.

### 352 3.3. Water temperature

353 The water temperature distribution of the tributary bay in different months is



354 shown in Fig. 7. From January to February, July to August, and October to December,  
355 the water temperatures in Zone 1 and Zone 2 were quite different. There was an  
356 obvious temperature boundary, which was mainly affected by the large difference  
357 between the upstream water temperature in the tributary bay and the backwater  
358 temperature from the main reservoir. From March to June and in September, the water  
359 temperature in Zone 1 was similar to that of Zone 2 due to the small difference  
360 between the water temperature at the tail of the tributary bay and the water  
361 temperature of the backwater from the main reservoir.



362  
363 **Fig. 7.** The vertical two-dimensional distribution of water temperature in different  
364 months. The black curve in the figure is the boundary between Zone 1 and Zone 2.

365 The surface water temperatures of the tributary bay in each month are shown in



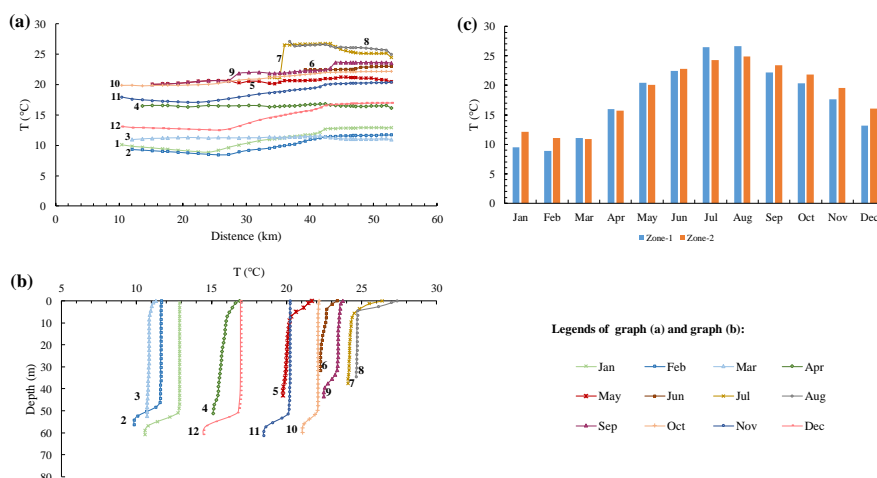
366 Fig. 8a. From March to June, due to the small difference between the upstream water  
367 temperature of the tributary bay and the backwater temperature of the main reservoir,  
368 the surface water temperature changed gently across the bay. The water temperature  
369 gradually decreased from the confluence to the tail of the tributary bay from July to  
370 August and gradually increased from September to October. The water temperature in  
371 the middle reaches was slightly lower than the temperature at the confluence and the  
372 tail of the tributary bay from January to February and from November to December.

373 The vertical water temperature in the confluence is shown in Fig. 8b. Affected by  
374 solar radiation and air temperature, the water temperature at the surface was relatively  
375 higher than that at the bottom (Zeng et al., 2016; Carey et al., 2012). The temperature  
376 in the middle layers changed little. There was a small thermocline in the surface water  
377 from May to August, and sinking of cold water occurred in January, February, and  
378 September to December.

379 The average water temperatures of Zone 1 and Zone 2 in different months are  
380 shown in Fig. 8c. The average water temperatures of Zone 1 and Zone 2 were similar  
381 from March to June and in September, while a difference of more than 1.5 °C existed  
382 in other months. As the water of Zone 1 mainly came from the upstream of the  
383 tributary bay, it was significantly affected by the air temperature (Mohseni and Stefan,  
384 1999). Zone 2 was mainly affected by the backwater from the main reservoir.  
385 Therefore, the average water temperature in Zone 1 was higher than that in Zone 2 in  
386 summer, and the average water temperature in Zone 1 was lower than that in Zone 2



387 in winter.



388

389 **Fig. 8.** Changes in water temperature. (a) The variation in surface water temperature  
390 in each month along the tributary bay, (b) the variation in the vertical water  
391 temperature at the confluence in each month, and (c) the average water temperatures  
392 of Zone 1 and Zone 2 in each month. The blue bar represents Zone 1, and the orange  
393 bar represents Zone 2 in panel (c).

### 394 3.4 Water quality

395 As shown in Fig. 9, the COD concentration in the tributary bay ranged from 0 - 13  
396 mg/L. There was no significant difference in COD concentrations between the tail of  
397 the tributary bay and the backwater from the main reservoir, both of which had values  
398 between 8 and 11 mg/L. With a decreasing trend along the bay, the concentration of  
399 COD reached a minimum value at the intersection of Zone 1 and Zone 2.

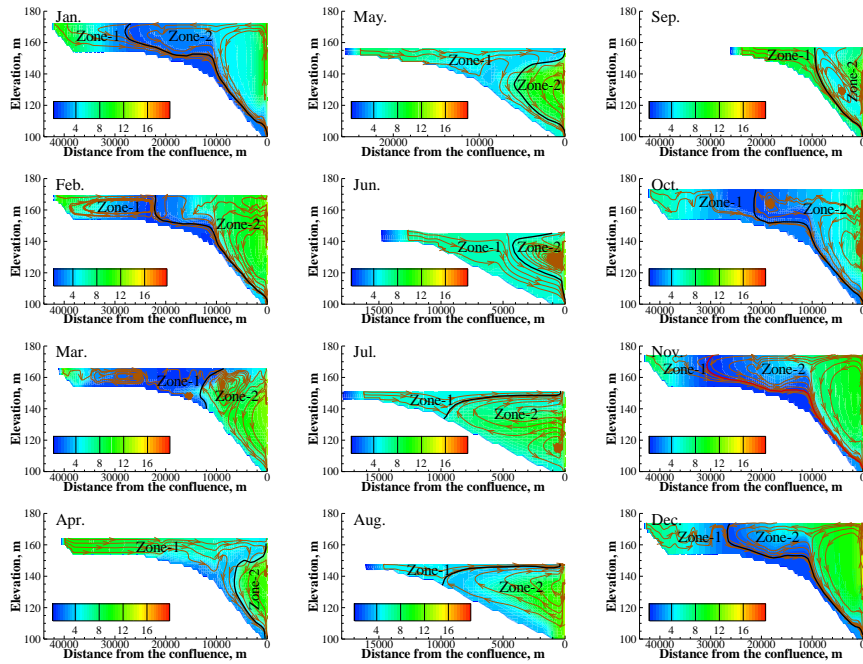
400 The  $\text{NH}_3\text{-N}$  concentration in the tributary bay was in the range of 0 - 0.3 mg/L  
401 (Fig. 10). Since the concentration of  $\text{NH}_3\text{-N}$  in the tail of the tributary bay was higher



402 than that of the backwater from the main reservoir, the concentration of  $\text{NH}_3\text{-N}$  in  
403 Zone 1 was higher than that in Zone 2 from January to March and July to December.  
404 There was no significant difference in  $\text{NH}_3\text{-N}$  between the tail of the tributary bay and  
405 the backwater from the main reservoir in April to June. Additionally, with a  
406 decreasing trend along the bay, the concentration of  $\text{NH}_3\text{-N}$  was lower at the  
407 intersection of Zones 1 and 2 than at the tail of the tributary bay or the confluence.

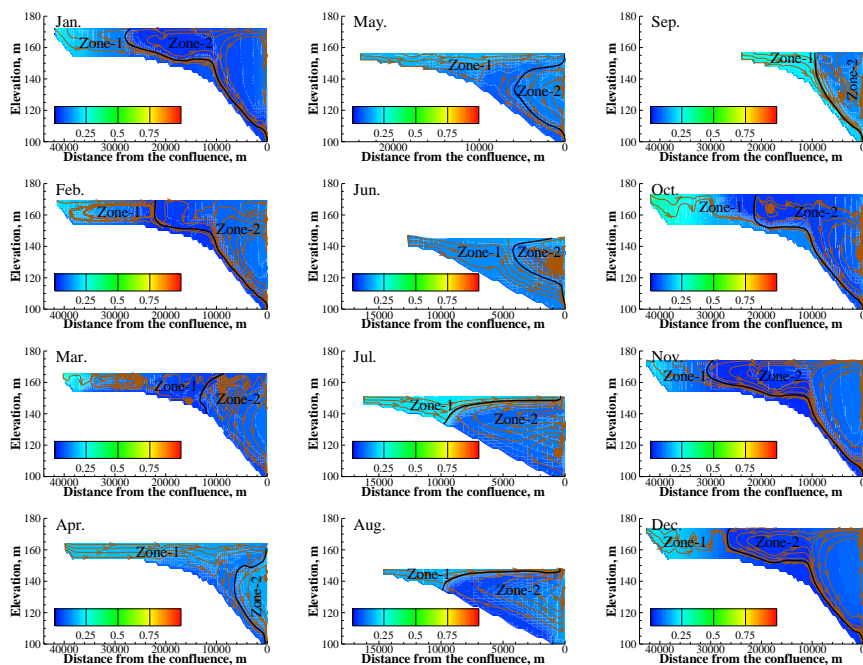
408 The distributions of TP and TN proved that the nutrients in tributary bays did not  
409 originate solely in the tributary bays but instead were mainly from the main reservoir  
410 and that the nutrient levels were different across seasons. The distributions of TP and  
411 TN in the tributary bay were almost the same. The concentration near the confluence  
412 was relatively high. With the mixing of the water from the tail of the tributary bay and  
413 the backwater from the main reservoir and with the degradation of water quality, the  
414 concentrations of TP and TN gradually decreased. In particular, the concentration of  
415 TP was in the range of 0.04 - 0.12 mg/L, and the concentration of TN was in the range  
416 of 0.8 - 2.1 mg/L. The concentrations of TP and TN in Zone 2 were higher than those  
417 in Zone 1. There was an obvious quality concentration boundary in the tributary bay,  
418 which was basically consistent with the regional boundary of the flow field.  
419 Furthermore, there was an obvious transition zone near the quality boundary in  
420 January to May and September to December, while the transition zone in June to  
421 August was very weak.





422

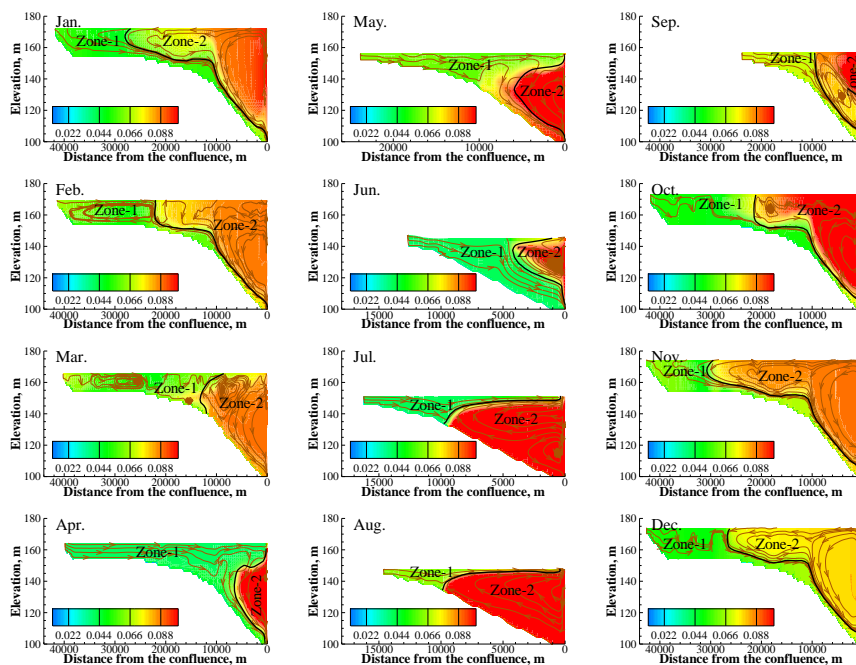
423 **Fig. 9.** The vertical two-dimensional distribution of COD in each month. The black  
424 curve in the figure is the boundary between Zone 1 and Zone 2.



425

426 **Fig. 10.** The vertical two-dimensional distribution of  $\text{NH}_3\text{-N}$  in each month. The black

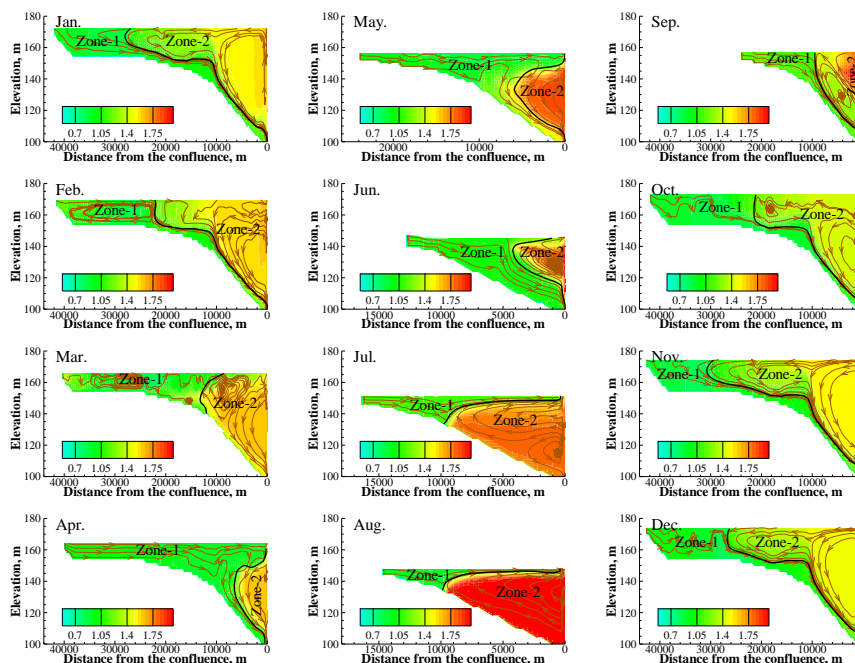
427 curve in the figure is the boundary between Zone 1 and Zone 2.



428

429 **Fig. 11.** The vertical two-dimensional distribution of TP in each month. The black

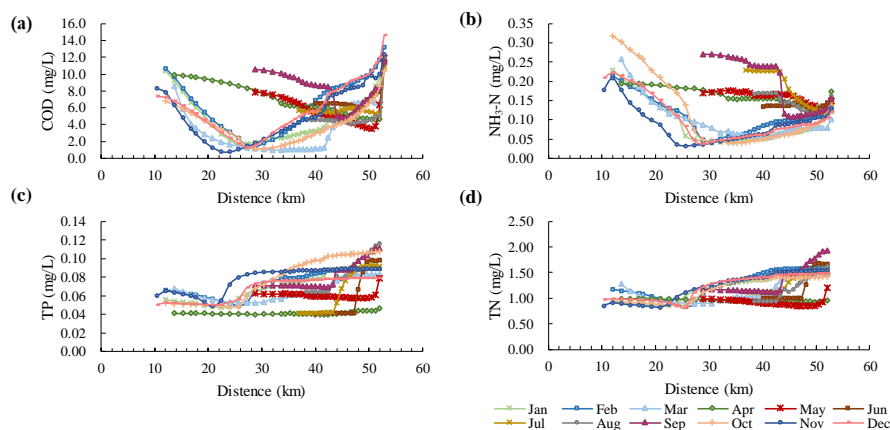
430 curve in the figure is the boundary between Zone 1 and Zone 2.



431

432 **Fig. 12.** The vertical two-dimensional distribution of TN in each month. The black  
433 curve in the figure is the boundary between Zone 1 and Zone 2.

434 The COD, NH<sub>3</sub>-N, TP and TN in the surface water of the tributary bay in different  
435 months are shown in Fig. 13. The concentrations of COD and NH<sub>3</sub>-N were generally  
436 higher on the two sides and lower in the middle. The concentrations of TP and TN  
437 were higher in the confluence and lower in the tail of the tributary bay.



438

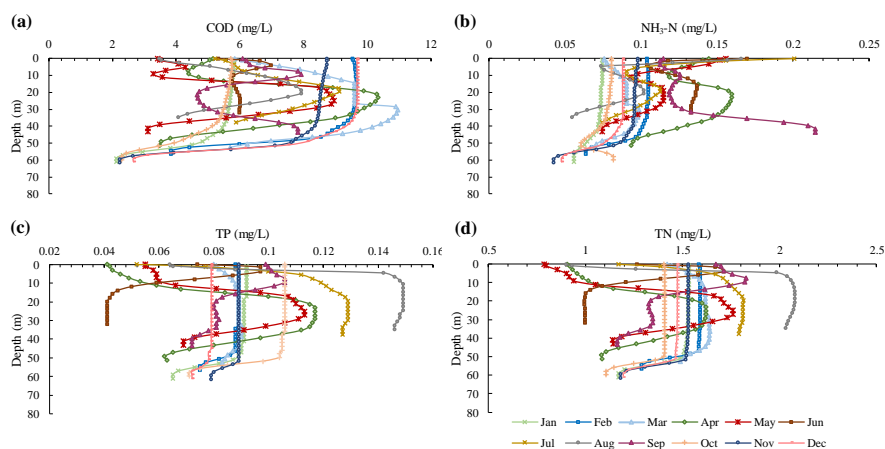
439 **Fig. 13.** The variation in surface water quality in different months along the tributary  
440 bay. (a) Variation in chemical oxygen demand, (b) variation in ammonia nitrogen, (c)  
441 variation in total phosphorus, and (d) variation in total nitrogen.

442 The vertical changes in COD,  $\text{NH}_3\text{-N}$ , TP and TN in different months at the  
443 confluence are shown in Fig. 14. There was no obvious regularity in the vertical water  
444 quality distributions of COD and  $\text{NH}_3\text{-N}$ . The average vertical variation in COD was  
445 4.6 mg/L over 12 months. The largest change appeared in December, with a value of  
446 7.0 mg/L, and the smallest change appeared in June, with a value of 1.6 mg/L. The  
447 average vertical variation in  $\text{NH}_3\text{-N}$  was 0.06 mg/L. The largest change appeared in  
448 January, with a value of 0.02 mg/L, and the smallest change appeared in July, with a  
449 value of 0.12 mg/L.

450 The concentrations of TP and TN were higher in the surface water and lower in  
451 the bottom in January to March and September to December, which was contrary to  
452 that in July and August. From April to June, the concentrations of TP and TN first

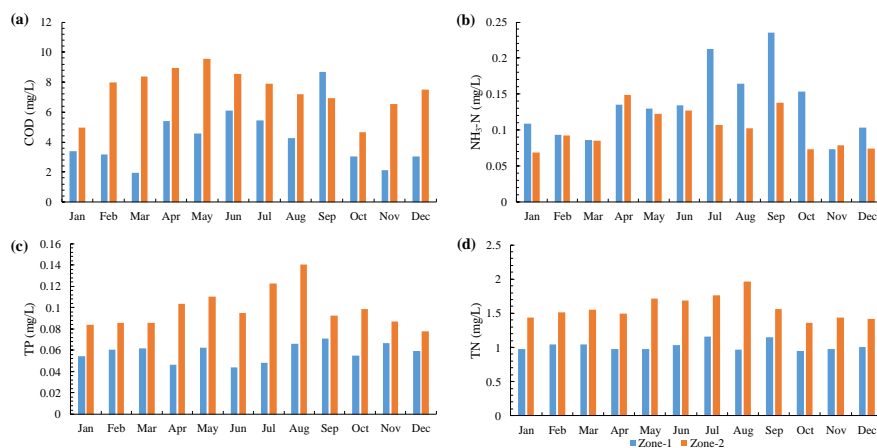


453 increased and then decreased from the surface to the bottom. The concentration  
454 gradient in the upper 10 m surface layer was relatively large.



455  
456 **Fig. 14.** The vertical variation in the water quality in different months at the section  
457 that was 6 km away from the confluence. (a) Variation in chemical oxygen demand, (b)  
458 variation in ammonia nitrogen, (c) variation in total phosphorus, and (d) variation in  
459 total nitrogen.

460 The average concentrations of COD, NH<sub>3</sub>-N, TP and TN in Zone 1 and Zone 2 are  
461 shown in Fig. 15. The COD concentration in Zone 2 was higher than that in Zone 1 in  
462 all months except September. The concentration of NH<sub>3</sub>-N in Zone 1 was higher than  
463 that in Zone 2 due to the higher concentration of NH<sub>3</sub>-N in the water of the tail of the  
464 tributary bay. For TP and TN, the concentrations in Zone 2 were higher than those in  
465 Zone 1.



466

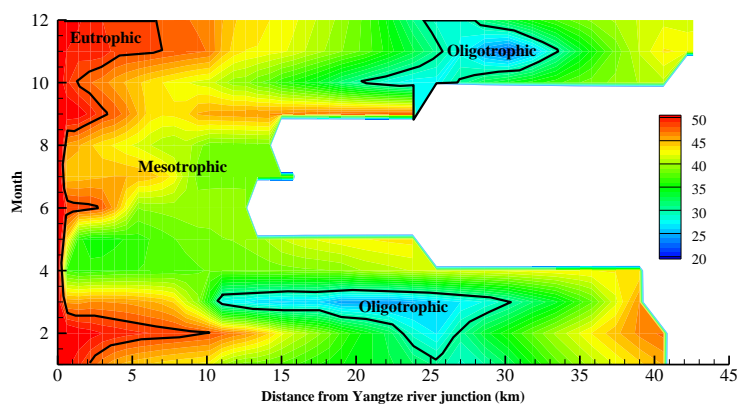
467 **Fig. 15.** The average water quality changes in Zone 1 and Zone 2. (a) Variation in  
468 chemical oxygen demand, (b) variation in ammonia nitrogen, (c) variation in total  
469 phosphorus, and (d) variation in total nitrogen. The blue bar represents Zone 1, and  
470 the orange bar represents Zone 2.

### 471 3.5 Water eutrophication

472 The distribution of the TLI( $\Sigma$ ) values in the surface water of the tributary bay in  
473 different months is shown in Fig. 16. The TLI( $\Sigma$ ) within 0.5 km of the confluence was  
474 relatively higher than in other areas throughout the year, reaching the level of light  
475 eutrophication. Additionally, the reach with high TLI( $\Sigma$ ) values in February and in  
476 September to December had a long range. From January to March and September to  
477 December, the reach approximately 25 km from the confluence had low TLI( $\Sigma$ )  
478 values, reaching oligotrophic status. In the rest of the time and area, the TLI( $\Sigma$ ) values  
479 correspond to a medium nutrient level. Additionally, the water temperature near the  
480 confluence was less than 20 °C, and the light conditions were poor in January to April



481 and November to December. Temperature and light conditions are important factors in  
482 the occurrence of eutrophication, and neither low temperatures nor poor light  
483 conditions are conducive to the growth of algae (Singh and Singh, 2015; Romarheim  
484 et al., 2015; Paerl et al., 2011; Reynolds, 2006). Physical dynamics play a critical role  
485 in estuarine biological production, material transport and water quality (Kasai et al.,  
486 2010). The results of this study showed that the tributary bay was mainly affected by  
487 backwater intrusion of the main reservoir in July and from August to October. During  
488 this time, the vertical mixing of water near the confluence was severe, which was also  
489 not conducive to the growth of algae (Gao et al., 2017; Lindim et al., 2011; Huisman  
490 et al., 2006). In conclusion, considering the influence of hydrodynamics, water  
491 temperature and water quality, the risk of eutrophication in the tributary bay was  
492 highest in the section within 0.5 km of the confluence from May to June.



493  
494 **Fig. 16.** Eutrophication results of surface water in the tributary bay. The nutrient  
495 status of the tributary bay is divided into three states (oligotrophic, mesotrophic and





496 eutrophic) according to the comprehensive nutrient index.

#### 497 **4 Conclusions and future work**

498 In this paper, the effect of the backwater jacking and intrusion of the main reservoir  
499 on the hydrodynamics and water environment of the Tangxi River, a tributary bay of  
500 the TGR are studied. The following conclusions were reached as a result of the  
501 research:

502 (1) The intrusion was weak when the water level of the main reservoir dropped,  
503 and the tributary bay was mainly affected by the backwater jacking of the main  
504 reservoir. Conversely, when the water level of the main reservoir rose, the tributary  
505 bay was mainly affected by backwater intrusion from the main reservoir. Since the  
506 backwater intrusion brought serve vertical mixing of water that was not conducive to  
507 the growth of algae, the controlling measures of eutrophication could contrapuntally  
508 be proposed in the time that the water level of the main reservoir dropped.

509 (2) The water from the tail flowed along the surface of the tributary bay or sank to  
510 the bottom in each month. The backwater from the main reservoir entered the  
511 confluence at different depths simultaneously, forming one or two circulations in the  
512 tributary bay. The backwater had a greater impact on the tributary bay when the main  
513 reservoir was at high water level and had a smaller impact when the main reservoir  
514 was at a low water level.

515 (3) The water temperature of the tributary bay was not greatly affected by the  
516 backwater from the main reservoir. The water qualities in different parts of the



517 tributary bay were quite different. The concentrations of COD and NH<sub>3</sub>-N in the  
518 tributary bay were generally higher at the two ends of the bay and lower in the middle.  
519 The concentrations of TP and TN were higher at the confluence and lower at the tail  
520 of the tributary bay. Moreover, for TP and TN, there was an obvious quality  
521 concentration boundary in the tributary bay, which was basically consistent with the  
522 regional boundary of the flow field. The concentrations of TP and TN were higher in  
523 the side near the confluence than that in the other side.

524 (4) Nutrients in tributary bays were mainly from the main reservoir and the  
525 nutrient levels were affected by constantly changing hydrodynamic conditions and  
526 environmental factors across seasons. According to the simulation of eutrophication,  
527 the TLI( $\Sigma$ ) values within 0.5 km of the confluence were relatively high. Considering  
528 the influence of hydrodynamics, water temperature and water quality, the risk of  
529 eutrophication of the tributary bay was high within 0.5 km of the confluence in May  
530 and June.

531 (5) Though the nutrients in tributary bays were mainly from the main reservoir,  
532 the backwater effect of the main reservoir didn't influence the water environment of  
533 the whole tributary bay. Therefore, we can focus on the areas that are more affected  
534 by the main reservoir and propose protective measures targeted at these areas.

535 This paper only studied the influence of the main reservoir on the tributary bay in  
536 terms of hydrodynamics and water environment. The influence of the tributary bay on  
537 the main reservoir and the interaction between the main reservoir and the tributary



538 bay are still unclear. In the future, numerical simulation of the main reservoir's  
539 hydrodynamics and water environment based on the results of this paper should be  
540 carried out to explore the interaction between the main reservoir and the tributary bay.

541 Future work should also explore control measures to improve the water  
542 environment of the tributary bay based on its interaction with the main reservoir. At  
543 present, some scholars have proposed that preventing and controlling eutrophication  
544 in tributary bays can be achieved by the method of "double nutrient reduction", which  
545 involves the simultaneous control of the nutrient inputs from the main stream and the  
546 tributary (Liang et al., 2014). It is also possible to use ecological methods, such as  
547 emergent plants, submerged plants, phytoplankton, benthic organisms and fish, to  
548 improve water eutrophication (Srivastava et al., 2017; Li et al., 2013; Soares et al.,  
549 2011). In addition, the concept of improving the hydrodynamic conditions of the main  
550 stream and controlling the eutrophication of the water body through manually  
551 controlled operation has been widely accepted by many experts and scholars (Yao,  
552 2011; Zheng et al., 2011; Naselli-Flores and Barone, 2005). Based on future research  
553 on the interaction between the main reservoir and the tributary bay with the goal of  
554 ensuring the main function of the main reservoir, water environment protection  
555 measures should be reasonably proposed for tributary bays in the future.

556 *Declaration of Competing Interest.* We declare that we have no known competing  
557 financial interests or personal relationships that could have appeared to influence the  
558 work reported in this paper.



559 *Acknowledgements.* This work was sponsored by the fund of Sichuan Province under  
560 permission number 2018SZYZF0001.

561 *Author contribution.* All co-authors participated in the field collection, data analysis,  
562 and/or writing of this manuscript. Ruifeng Liang was primarily responsible for  
563 preparation and process of this manuscript. Xintong Li and Yuanming Wang  
564 conceived of the study design and data analysis with input from all co-authors.

#### 565 **References**

566 Bennett, M. G., Schofield, K. A., Lee, S. S. and Norton, S. B.: Response of  
567 chlorophyll a to total nitrogen and total phosphorus concentrations in lotic  
568 ecosystems: a systematic review protocol, *Environmental Evidence*, 6(1), 18,  
569 <https://doi.org/10.1186/s13750-017-0097-8>, 2017.

570 Bockelmann, B. N., Fenrich, E. K., Lin, B. and Falconer, R. A.: Development of an  
571 ecohydraulics model for stream and river restoration, *Ecological Engineering*,  
572 22(4-5), 227-235, <https://doi.org/10.1016/j.ecoleng.2004.04.003>, 2004.

573 Cai, Q. and Hu, Z.: Studies on eutrophication problem and control strategy in the  
574 Three Gorges Reservoir, *Acta Hydrobiologica Sinica*, 30(1), 7-11 (in Chinese),  
575 <https://doi.org/10.3321/j.issn:1000-3207.2006.01.002>, 2006.

576 Carey, C. C., Ibelings, B. W., Hoffmann, E. P., Hamilton, D. P. and Brookes, J. D.:  
577 Eco-physiological adaptations that favour freshwater cyanobacteria in a changing  
578 climate, *Water Research*, 46(5), 1394-1407,  
579 <https://doi.org/10.1016/j.watres.2011.12.016>, 2012.



- 580 Carlson, R. E.: A trophic state index for lakes. *Limnology and Oceanography*, 22(2),  
581 361-369, <https://doi.org/10.4319/lo.1977.22.2.0361>, 1977.
- 582 Debele, B., Srinivasan, R. and Parlange, J. Y.: Coupling upland watershed and  
583 downstream waterbody hydrodynamic and water quality models (SWAT and  
584 CE-QUAL-W2) for better water resources management in complex river basins,  
585 *Environmental Modeling & Assessment*, 13(1), 135-153,  
586 <https://doi.org/10.1007/s10666-006-9075-1>, 2008.
- 587 Deng, S. and Bai, Y.: Analysis on the role of environmental impact assessment in the  
588 construction of water conservancy and hydropower projects, *Environment and  
589 Sustainable Development*, 41(5), 101-102 (in Chinese),  
590 <https://doi.org/10.19758/j.cnki.issn1673-288x.2016.05.030>, 2016.
- 591 Fang, J.: The Operating Simulation of Cascade Reservoirs and it's Impacts on River  
592 Eco-environment—A Case Study on Upper reaches of the Yangtze River. Ph.D,  
593 Institute of Mountain Hazards and Environment Chinese Academy of Sciences,  
594 2007.
- 595 Feng, J., Li, R., Liang, R. and Shen, X.: Eco-environmentally friendly operational  
596 regulation: an effective strategy to diminish the TDG supersaturation of reservoirs,  
597 *Hydrology and Earth System Sciences*, 18, 1213-1223,  
598 <https://doi.org/10.5194/hess-18-1213-2014>, 2014.
- 599 Gao, Q., He, G., Fang, H. and Huang, L.: Effects of vertical mixing on algal growth in  
600 the tributary of Three Gorges Reservoir, *Journal of Hydraulic Engineering* 48(1),



- 601 96-103 (in Chinese), <https://doi.org/10.13243/j.cnki.slxh.20160239>, 2017.
- 602 Gao, X., Zeng, Y., Wang, J. and Liu, H.: Immediate impacts of the second  
603 impoundment on fish communities in the Three Gorges Reservoir, Environmental  
604 Biology of Fishes, 87, 163-173, <https://doi.org/10.1007/s10641-009-9577-1>, 2010.
- 605 Holbach, A., Bi, Y., Yuan, Y., Wang, L., Zheng, B. and Norra, S.: Environmental water  
606 body characteristics in a major tributary backwater of the unique and strongly  
607 seasonal Three Gorges Reservoir, China, Environmental Science Processes:  
608 Processes & Impacts, 17(9), 1641-1653, <https://doi.org/10.1039/C5EM00201J>,  
609 2015.
- 610 Holbach, A., Norra, S., Wang, L. Yuan, Y., Wei, H. and Zheng, B.: Three Gorges  
611 Reservoir: Density Pump Amplification of Pollutant Transport into Tributaries,  
612 Environmental Science & Technology, 48(14), 7798-7806,  
613 <https://doi.org/10.1021/es501132k>, 2014.
- 614 Hu B., Yang Z., Wang, H., Sun, X., Bi, N. and Li, G.: Sedimentation in the Three  
615 Gorges Dam and the future trend of Changjiang (Yangtze River) sediment flux to  
616 the sea, Hydrology and Earth System Sciences, 13, 2253-2264,  
617 <https://doi.org/10.5194/hess-13-2253-2009>, 2009.
- 618 Huisman, J., Pham Thi, N. N., Karl, D. M. and Sommeijer, B.: Reduced mixing  
619 generates oscillations and chaos in the oceanic deep chlorophyll maximum,  
620 Nature, 439(7074), 322-325, <https://doi.org/10.1038/nature04245>, 2006.
- 621 Ji, D., Wells, S. A., Yang, Z., Liu, D., Huang, Y., Ma, J. and Chris, J. B.: Impacts of



- 622 water level rise on algal bloom prevention in the tributary of Three Gorges  
623 Reservoir, China, Ecological Engineering, 98, 70-81,  
624 <https://doi.org/10.1016/j.ecoleng.2016.10.019>, 2017.
- 625 Kasai, A., Kurikawa, Y., Ueno, M., Robert, D., and Yamashita, Y.: Salt-wedge  
626 intrusion of seawater and its implication for phytoplankton dynamics in the Yura  
627 Estuary, Japan, Estuarine, Coastal and Shelf Science, 86(3), 408-414,  
628 <https://doi.org/10.1016/j.ecss.2009.06.001>, 2010.
- 629 Lewis, W. M., Wurtsbaugh, W. A. and Paerl, H. W.: Rationale for control of  
630 anthropogenic nitrogen and phosphorus to reduce eutrophication of inland waters,  
631 Environmental Science & Technology, 45(24), 10300-10305,  
632 <https://doi.org/10.1021/es202401p>, 2011.
- 633 Li, K., He, W., Hu, Q. and Gao, S.: Ecological restoration of reclaimed wastewater  
634 lakes using submerged plants and zooplankton, Water and Environment Journal,  
635 28(3), 323-328, <https://doi.org/10.1111/wej.12038>, 2013.
- 636 Li, Z. and Zhang, H.: Trophic State Index and its Correlation with Lake Parameters in  
637 China, Acta Scientiae Circumstantiae, 13(4), 391-397 (in Chinese),  
638 <https://doi.org/10.13671/j.hjkxxb.1993.04.002>, 1993.
- 639 Liang, L., Deng, Y., Zheng, M. and Wei, X.: Predicting of Eutrophication in the  
640 Longchuan River Based on CE-QUAL-W2 Model, Resources and Environment in  
641 the Yangtze Basin, 23(1), 103-111, <https://doi.org/10.11870/cjlyzyyhj2014Z1015>,  
642 2014.



- 643 Lindim, C., Pinho, J. L. and Vieira, J. M. P.: Analysis of spatial and temporal patterns  
644 in a large reservoir using water quality and hydrodynamic modeling, *Ecological*  
645 *Modelling*, 222(14), 2485-2494, <https://doi.org/10.1016/j.ecolmodel.2010.07.019>,  
646 2011.
- 647 Liu, D., Yang, Z., Ji, D., Ma, J. and Cui, Y.: A review on the mechanism and its  
648 controlling methods of the algal blooms in the tributaries of Three Gorges  
649 Reservoir, *Journal of Hydraulic Engineering*, 47(03), 443-454 (in Chinese),  
650 <https://doi.org/10.13243/j.cnki.slxh.20151304>, 2016.
- 651 Liu, L.: Effects of vertical mixing on phytoplankton blooms in Xiangxi Bay of Three  
652 Gorges Reservoir: Implications for management, *Water Research*, 46(07),  
653 2121-2130, <https://doi.org/10.1016/j.watres.2012.01.029>, 2012.
- 654 Long, L., Ji, D., Yang, Z., Ma, J., Scott, A. W., Liu, D. and Andreas, L.: Density -  
655 driven water circulation in a typical tributary of the Three Gorges Reservoir,  
656 China, *River Research and Application*, 35(7), 1-11,  
657 <https://doi.org/10.1002/rra.3459>, 2019.
- 658 Long, L., Xu H., Bao, Z., Ji, D. and Liu, D.: Temporal and spatial characteristics of  
659 water temperature in Xiluodu Reservoir, *Journal of Hydroelectric Engineering*,  
660 37(4), 79-89 (in Chinese), <https://doi.org/10.11660/slfdb.20180408>, 2018.
- 661 Lu, Q., Li, R., Li, J., Li, K. and Wang, L.: Experimental study on total dissolved gas  
662 supersaturation in water, *Water Science and Engineering*, 04(4), 396-404,  
663 <https://doi.org/10.3882/j.issn.1674-2370.2011.04.004>, 2011.





- 664 McGrath, K. E., Dawley, E. M. and Geist, D. R.: Total Dissolved Gas Effects on  
665 Fishes of the Lower Columbia River, PNNL-15525, Pacific Northwest National  
666 Laboratory, Richland, Washington, <https://doi.org/10.2172/918864>, 2006.
- 667 Mohseni, O. and Stefan, H. G.: Stream temperature/air temperature relationship: a  
668 physical interpretation, Journal of Hydrology, 218(3), 128-141,  
669 [https://doi.org/10.1016/S0022-1694\(99\)00034-7](https://doi.org/10.1016/S0022-1694(99)00034-7), 1999.
- 670 Morgenstern, U., Daughney, C. J., Leonard, G., Gordon, D., Donath, F. M., and  
671 Reeves, R.: Using groundwater age and hydrochemistry to understand sources and  
672 dynamics of nutrient contamination through the catchment into Lake Rotorua,  
673 New Zealand, Hydrology and Earth System Sciences, 19, 803-822,  
674 <https://doi.org/10.5194/hess-19-803-2015>, 2015.
- 675 Naselli-Flores, L. and Barone, R.: Water-Level Fluctuations in Mediterranean  
676 Reservoirs: Setting a Dewatering Threshold as a Management Tool to Improve  
677 Water Quality, Hydrobiologia, 548, 85-99,  
678 <https://doi.org/10.1007/s10750-005-1149-6>, 2005.
- 679 Noori, R., Yeh, H. D., Ashrafi, K., Rezazadeh, N., Bateni, S. M., Karbassi, A.,  
680 Kachoosangi, F. T. and Moazami, S.: A reduced-order based CE-QUAL-W2  
681 model for simulation of nitrate concentration in dam reservoirs, Journal of  
682 Hydrology, 530, 645-656, <https://doi.org/10.1016/j.jhydrol.2015.10.022>, 2015.
- 683 Oldani, N. O. and Claudio R. M. Baigún: Performance of a fishway system in a major  
684 South American dam on the Parana River (Argentina–Paraguay), River Research



- 685 and Application, 18(2), 171-183, <https://doi.org/10.1002/rra.640>, 2002.
- 686 Paerl, H. W., Hall, N. S. and Calandrino, E. S.: Controlling harmful cyanobacterial  
687 blooms in a world experiencing anthropogenic and climatic-induced change,  
688 Science of the Total Environment, 409(10), 1739-1745,  
689 <https://doi.org/10.1016/j.scitotenv.2011.02.001>, 2011.
- 690 Pan, X., Tang, L., Feng, J., Liang, R., Pu, X., Li, R., and Li, K.: Experimental  
691 Research on the Degradation Coefficient of Ammonia Nitrogen Under Different  
692 Hydrodynamic Conditions, Bulletin of Environmental Contamination and  
693 Toxicology, 104, 288, <https://doi.org/10.1007/s00128-019-02781-0>, 2020.
- 694 Peng, C., Chen, L., Bi, Y., Xia, C., Lei, Y., Yang, Y., Jian, T. and Hu, Z.: Effects of  
695 flood regulation on phytoplankton community structure in the Xiangxi River, a  
696 tributary of the Three Gorges Reservoir, China Environmental Science, 34,  
697 1863-1871, <https://doi.org/10.1097/NEN.000000000000183>, 2014.
- 698 Ran, X., Alexander, F. B., Yu, Z. and Liu, J.: Implications of eutrophication for  
699 biogeochemical processes in the Three Gorges Reservoir, China, Regional  
700 Environmental Change, 19(1), 55-63, <https://doi.org/10.1007/s10113-018-1382-y>,  
701 2019.
- 702 Reynolds, C. S.: The ecology of phytoplankton, Cambridge University Press, London,  
703 2006.
- 704 Romarheim, A. T., Tominaga, K., Riise, G., and Andersen, T.: The importance of  
705 year-to-year variation in meteorological and runoff forcing for water quality of a



- 706 temperate, dimictic lake, Hydrology and Earth System Sciences, 19, 2649-2662,  
707 <https://doi.org/10.5194/hess-19-2649-2015>, 2015.
- 708 Singh, S. P. and Singh, P.: Effect of temperature and light on the growth of algae  
709 species: A review, Renewable and Sustainable Energy Reviews, 50, 431-444,  
710 <https://doi.org/10.1016/j.rser.2015.05.024>, 2015.
- 711 Soares, M., Vale, M. and Vasconcelos, V.: Effects of nitrate reduction on the  
712 eutrophication of an urban man-made lake (Palácio de Cristal, Porto, Portugal),  
713 Environmental Technology, 32(9), 1009-1015,  
714 <https://doi.org/10.1080/09593330.2010.523437>, 2011.
- 715 Srivastava, A., Chun, S. J., Ko, S. R., Kim, J., Ahn, C. Y. and Oh, H-M.: Floating  
716 rice-culture system for nutrient remediation and feed production in a eutrophic  
717 lake, Journal of Environmental Management, 203, 342-348,  
718 <https://doi.org/10.1016/j.jenvman.2017.08.006>, 2017.
- 719 Tang, Q., Bao, Y., He, X., Fu, B., Adrian, L. C. and Zhang, X.: Flow regulation  
720 manipulates contemporary seasonal sedimentary dynamics in the reservoir  
721 fluctuation zone of the Three Gorges Reservoir, China, Science of the Total  
722 Environment, 548-549: 410-420, <https://doi.org/10.1016/j.jenvman.2017.08.006>,  
723 2016.
- 724 Thomas, M. C. and Scott A. W.: CE-QUAL-W2: A two-dimensional laterally  
725 averaged hydrodynamic and water quality model, Version 3.6, Department of  
726 Civil and Environmental Engineering, Portland State University, Portland, 2008.



- 727 Wang, Q.: Influence on fishes of dissolved gas supersaturation caused by high-dam  
728 discharging and its countermeasures, Proceedings of 2011 International  
729 Symposium on Water Resource and Environmental Protection, Xi'an,  
730 <https://doi.org/10.1109/ISWREP.2011.5893398>, 2011.
- 731 Wang, R., Huang, T. and Wu, W.: Different factors on nitrogen and phosphorus  
732 self-purification ability from an urban Guandu-Huayuan river, Journal of Lake  
733 Sciences, 28(1), 105-113, <https://doi.org/10.18307/2016.0112>, 2016.
- 734 Wu, W.: Change of Channel Conditions of the Reach from Wanzhou to Fuling in the  
735 Yangtze River at Incipient Stage of Three Gorges Reservoir, Journal of Chongqing  
736 Jiaotong University (Natural Science), 32(3), 475-479 (in Chinese),  
737 <https://doi.org/10.3969/j.issn.1674-0696.2013.03.25>, 2013.
- 738 Xiong, C., Liu, D., Zheng, B., Zhang, J., Hu, N., Zhang, Y. and Chen, Y.: The  
739 Influence of Hydrodynamic Conditions on Algal Bloom in the Three Gorges  
740 Reservoir Tributaries, Applied Mechanics and Materials, 295-298, 1981-1990,  
741 <https://doi.org/10.4028/www.scientific.net/amm.295-298.1981>, 2013.
- 742 Yang, Z., Cheng, B., Xu, Y., Liu, D., Ma, J. and Ji, D.: Stable isotopes in water  
743 indicate sources of nutrients that drive algal blooms in the tributary bay of a  
744 subtropical reservoir, Science of The Total Environment 634, 205-213,  
745 <https://doi.org/10.1016/j.scitotenv.2018.03.266>, 2018.
- 746 Yang, Z., Liu, D., Ji, D. and Xiao, S.: Influence of the impounding process of the  
747 Three Gorges Reservoir up to water level 172.5 m on water eutrophication in the



- 748 Xiangxi Bay, Science China Technological Sciences 53(4), 1114-1125,  
749 <https://doi.org/10.1007/s11431-009-0387-7>, 2010.
- 750 Yao, X., Liu, D., Yang, Z., Ji, D. and Fang, X.: Preliminary Studies on the Mechanism  
751 of Winer Dinoflagellate Bloom in Xiangxi Bay of the Three Gorges Reservoir,  
752 Research of Environmental Sciences, 25(6), 645-651 (in Chinese),  
753 <https://doi.org/10.13198/j.res.2012.06.40.yaoxj.001>, 2012.
- 754 Yin, W., Ji, D., Hu, N., Xie, T., Huang, Y., Li, Y. and Zhou J.: Three-dimensional  
755 Water Temperature and Hydrodynamic Simulation of Xiangxi River Estuary,  
756 Advanced Materials Research, 726-731(2013), 3212-3221,  
757 <https://doi.org/10.4028/www.scientific.net/AMR.726-731.3212>, 2013.
- 758 Yu, Z., Wang, L., Zhang, L., Yang Y., Yan, L., Zhang, J. and Yang, Y.: Hydrodynamic  
759 characteristics in a valley type tributary bay during the raising and falling  
760 temperature periods, Applied Mechanics and Materials, 353-356(2013),  
761 2567-2571, <https://doi.org/10.4028/www.scientific.net/AMM.353-356.2567>,  
762 2013.
- 763 Zeng, M., Huang, T., Qiu, X., Wang, Y., Shim J., Zhou, S. and Liu, F.: Seasonal  
764 Stratification and the Response of Water Quality of a Temperate  
765 Reservoir—Zhoucun Reservoir in North of China, Environmental Science, 37(4):  
766 1337-1344 (in Chinese), <https://doi.org/10.13227/j.hjcx.2016.04.019>, 2016.
- 767 Zhang, H.: Ways to effectively improve the design level of water conservancy and  
768 hydropower projects, China Science and Technology Information 5, 89-90 (in



- 769 Chinese), <https://doi.org/10.3969/j.issn.1001-8972.2014.05.024>, 2014.
- 770 Zhang, S., Song, D., Zhang, K., Zeng, F. and Li, D.: Trophic status analysis of the  
771 upper stream and backwater area in typical tributaries, Three Gorges Reservoir,  
772 Journal of Lake Sciences, 22 (2), 201-207 (in Chinese),  
773 <https://doi.org/10.1017/S0004972710001772>, 2010.
- 774 Zheng, B., Zhao, Y., Qin, Y., Ma, Y. and Han, C.: Input characteristics and sources  
775 identification of nitrogen in the three main tributaries of the Three Gorges  
776 Reservoir, China, Environmental Earth Sciences, 75(17): 1219,  
777 <https://doi.org/10.1007/s12665-016-6028-0>, 2016.
- 778 Zheng, T.: The Study of Water Environment and Sedimentation Regimes in the Upper  
779 Three Gorges Reservoir. Proceedings of 2011 International Symposium on Water  
780 Resource and Environmental Protection, Xi'an,  
781 <https://doi.org/10.1109/ISWREP.2011.5893641>, 2011.
- 782 Zheng, T., Mao J., Dai H. and Liu D.: Impacts of water release operations on algal  
783 blooms in a tributary bay of Three Gorges Reservoir, Science China  
784 (Technological Sciences), 54(6), 1588-1598,  
785 <https://doi.org/10.1007/s11431-011-4371-7>, 2011.
- 786 Zhou, J., Zhang M. and Lu, P.: The effect of dams on phosphorus in the middle and  
787 lower Yangtze river, Water Resource Research, 49, 3659-3669,  
788 <https://doi.org/10.1002/wrcr.20283>, 2013.
- 789 Zhu, S.: Preliminary Study on Physical Characteristics of Sediment Deposition in the



790 Three Gorges Reservoir, MA.Sc. Changjiang River Scientific Research Institute  
791 (in Chinese), 2017.

792 Ziv, G., Baran, E., Nam, S., Rodriguez-Iturbe, I. and Levin, S. A.: Trading-off fish  
793 biodiversity, food security, and hydropower in the Mekong River Basin,  
794 Proceedings of the National Academy of Sciences of the United States of America,  
795 109 (15), 5609-5614. <https://doi.org/10.1073/pnas.1201423109>, 2012.

796 Zou, J. and Zhai, H.: Impacts of Three Gorges Project on water environment and  
797 aquatic ecosystem and protective measures, Water Resources Protection, 32(05),  
798 136-140 (in Chinese), <https://doi.org/10.3880/j.issn.1004-6933.1016.05.025>,  
799 2016.